An Unusual Coordination Mode for Amides: Lone-Pair Binding via Nitrogen

Jesse C. Lee, Jr., Beat Müller, Paul Pregosin,* Glenn P. A. Yap, Arnold L. Rheingold,* and Robert H. Crabtree*

Department of Chemistry, Yale University, New Haven, Connecticut 06520, Department of Chemistry, University of Delaware, Newark, Delaware 19716, and ETH, Zürich, Switzerland

Received December 29, 1994[⊗]

A variety of 8-amino- and amido-substituted quinolines react with $[Ir(PPh_3)_2H_2(acetone)_2]SbF_6$ (**1**) to give a series of complexes in which the amine or amide nitrogen binds to the metal. The X-ray crystal structures of $[Ir(H)_2(PPh_3)_2(C_9H_6N\{HNCO^tBu\})]SbF_6$ (**4b**) and $[Ir(H)_2(PPh_3)_2(C_9H_6N\{HNSi^tBuMe_2\})]SbF_6$ (**4c**) were obtained: **4b**, $a = 9.904(4)$ Å, $b = 13.480(5)$ Å, $c = 19.346(9)$ Å, $\alpha = 83.79(4)°$, $\beta = 81.64\ (4)°$, $\gamma = 76.52(3)°$, $Z = 2$, triclinic $P\bar{1}$, $R = 5.37\%$; **4c**, $a = 45.24(1)$ Å, $b = 10.536(3)$ Å, $c = 25.450(7)$ Å, $\beta = 111.11(2)°$, $Z = 8$, monoclinic $C2/c$, $R = 5.30\%$. The X-ray data do not allow a definite distinction between the two possible binding modes, N binding via the lone pair and N−H agostic (2e, 3-center) binding. Definitive evidence for the lone-pair-bound structure was obtained from natural-abundance ^{15}N heteronuclear multiple-quantum coherence (HMQC) spectroscopy and proton nuclear Overhauser effect (NOE) data. The amine or amide N therefore rehybridizes to sp^3 on binding, a previously unreported complexation mode for undeprotonated amides that normally coordinate via O. Fluxional exchange processes are interpreted on the basis of N lone-pair decoordination and inversion with the possible intermediacy of an agostic species or iminol tautomer. The Ir−N bond distances (**4b**, 2.313(9) Å and **4c**, 2.320(10) Å) are very long. The NH of the coordinated amide is much more acidic than that of the free amide and can be deprotonated with NEt_3 to give an N-bound complex of the deprotonated amide. In a conformationally restricted pyrrole where the N lone pair cannot bind to Ir, we find that deprotonation occurs spontaneously to give a pyrrolyl complex.

I. Introduction

The agostic[1a−c] (2e, 3-center) binding of X−H bonds to transition metals has attracted intense interest in connection with the problem of σ bond activation.[2] In such complexes the X−H bonding pair is donated to the metal to give a species in which the X−H is bound side-on to the metal. Many cases are known[3] for which X is H, C, B, and Si, but examples for other X−H bonds are rare. We were curious as to what would happen in the case of an N−H bond, where in principle the metal has a choice between a N lone pair and N−H agostic binding. Several cases of N−H···M (d^8 or d^{10}) binding have been observed. In the d^8 square planar system,[4] the N−H approaches in the out-of-plane ($\pm z$) direction. A nonbonding electron pair is available along this direction, so this is probably a 3-center, 4-electron bond (hydrogen bond). In the d^{10} system, which has no low-lying empty orbitals to accept electrons, the N−H···M interaction is clearly a hydrogen bond.

In a d^6-ML_5 system, such as is formed by loss of an acetone from $[Ir(PPh_3)_2H_2(acetone)_2]^+$ (**1**), an empty orbital is available at the sixth site, allowing the choice between N−H agostic binding or N lone-pair binding. The iridium system is already known[5] to readily form σ bond complexes with H_2, C−H, and Si−H bonds. To favor N−H agostic binding as much as possible, we chose an 8-aminoquinoline system of type **2**, where the N lone pair is already somewhat deactivated by conjugation with the adjacent aromatic group. In addition, we incorporated acyl (**2b** and **d**) and silyl substituents (**2c**) to further deactivate the N lone pair.

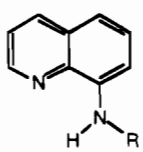

2 (R = H, **a**; CO^tBu, **b**; $SiMe_2tBu$, **c**; COMe, **d**)

In our first attempt,[6a] we found that quinoline-8-acetamide (**2d**) tautomerizes to the very rare iminol form, which binds to $[Ir(PPh_3)_2H_2(acetone)_2]SbF_6$ (**1**) via the N lone pair. This complex (**3**) was also of interest in that the iminol OH was found to form an unconventional hydrogen bond to the adjacent Ir−H group, an area we have now intensively investigated.[6b] This work gave evidence for an intermediate (eq 1), which we thought

[⊗] Abstract published in *Advance ACS Abstracts,* November 1, 1995.

(1) (a) Brookhart, M.; Green, M. L. H. *J. Organomet. Chem.* **1983**, *250*, 395. (b) Brookhart, M.; Green, M. L. H. *Prog. Inorg. Chem.* **1988**, *36*, 1. (c) Crabtree, R. H. *Angew. Chem., Int. Ed. Engl.* **1993**, *32*, 789.

(2) Crabtree, R. H. *Chem. Rev.* **1985**, *85*, 245.

(3) (a) Kubas, G. J.; Ryan, R. R.; Swanson, B. I.; Vergamini, P. J.; Wasserman, H. J. *J. Am. Chem. Soc.* **1984**, *100*, 451. (b) Kubas, G. J. *Acc. Chem. Res.* **1988**, *21*, 120. (c) Krauledat, H.; Brintzinger, H. H. *Angew. Chem.* **1990**, *102*, 1459; *Angew. Chem., Int. Ed. Engl.* **1990**, *29*, 1412. (d) Piers, W. E.; Bercaw, J. E. *J. Am. Chem. Soc.* **1990**, *112*, 9406. (e) Clawson, L.; Soto, J.; Buchwald, S. L.; Steigerwald, M. L.; Grubbs, R. H. *J. Am. Chem. Soc.* **1985**, *107*, 3377. (f) Fellman, J. D.; Schrock, R. R.; Traficante, D. D. *Organometallics* **1982**, *1*, 481. (g) James, B. D.; Wallbridge, M. G. Prog. *Inorg. Chem.* **1970**, *11*, 99. (h) Schubert, U. *Adv. Organomet. Chem.* **1990**, *30*, 151.

(4) (a) Brammer, L.; Charnock, J. M.; Goggin, P. L.; Goodfellow, R. J.; Orpen, A. G.; Koetzle, T. F. *J. Chem. Soc., Dalton Trans.* **1991**, 1789, and references therein. (b) Albinati, A.; Lianza, F.; Müller, B.; Pregosin, P. S. *Inorg. Chim. Acta* **1993**, *208*, 119. (c) Blake, A. J.; Holder, A. J.; Roberts, Y. V.; Schroder, M. *J. Chem. Soc., Chem. Commun.* **1993**, 260.

(5) (a) Crabtree, R. H.; Holt, E. M.; Lavin, M. E.; Morehouse, S. M. *Inorg. Chem.* **1985**, *24*, 1968. (b) Crabtree, R. H.; Lavin, M. *Chem. Comm.* **1985**, 794. (c) Luo, X.-L.; Crabtree, R. H. *J. Am. Chem. Soc.* **1989**, *111*, 2527.

(6) (a) Lee, J. C., Jr.; Rheingold, A. L.; Müller, B.; Pregosin, P.; Crabtree, R. H. *J. Chem. Soc., Chem. Commun.* **1994**, 1021. (b) Lee, J. C., Jr.; Peris, E.; Rheingold, A. L.; Crabtree, R. H. *J. Am. Chem. Soc.* **1994**, *116*, 11014.

0020-1669/95/1334-6295$09.00/0

might either be an N−H agostic or a lone-pair-bound species. Since neither type of complex is known, we have also followed up this problem and now report the isolation of stable analogs of the intermediate. Interestingly, X-ray crystallography was insufficient for characterization. However, natural-abundance ^{15}N heteronuclear multiple-quantum coherence (HMQC) and ^1H nuclear Overhauser effect spectrometry (NOESY) studies gave definitive evidence that the species all have lone-pair-bound sp^3 nitrogens.

II. Results and Discussion

Synthesis. In the case of **2d** the reaction sequence shown in eq 1 was previously established.

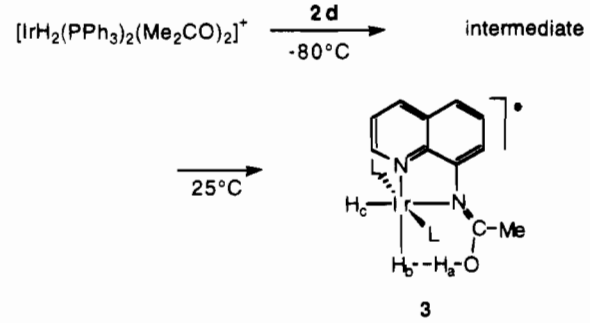

3

In order to probe the nature of the intermediate, we studied amide **2b** in which we thought the steric bulk of the *tert*-butyl group should avoid formation of the H-bonded species **3** by preventing the N−C bond rotation required to put the *tert*-butyl group *anti* to the metal. We now find that **2b** indeed forms a complex having an NMR spectrum similar to that of the intermediate but that this species is now stable on warming to room temperature and above.

For comparison to **3**, a series of related complexes was prepared from $[IrH_2(acetone)_2(PPh_3)_2]SbF_6$ (**1**) and the 8-substituted quinolines, **2a**, **2b**, and **2c**, in CH_2Cl_2 at 25 °C to give $[IrH_2(C_9H_6N\{NHR\})(PPh_3)_2]SbF_6$ (**4**) (R = H, **4a**; R = CO(^{t}Bu), **4b**; R = $SiMe_2(^t$Bu), **4c**). The complexes were obtained as crystalline solids and fully characterized as discussed below.

Reactivity. Compound **4b** loses a proton much more readily than does the free amide, and addition of NEt_3 gives the conventional deprotonated amide complex **5**, $[IrH_2(C_9H_6N\{NC(O)^tBu\})(PPh_3)_2]$, as shown by microanalytical and spectroscopic data. In particular, the complex shows one phosphorus signal at 21.12 ppm in the ^{31}P NMR and two triplets of doublets in the ^1H NMR at −18.97 and −21.68 ppm, with $^2J(^1H,^{31}P)_{cis}$ = 18.0 Hz and $^2J(^1H,^1H)_{cis}$ = 7.2 Hz, as expected for the inequivalent hydrides of **5**.

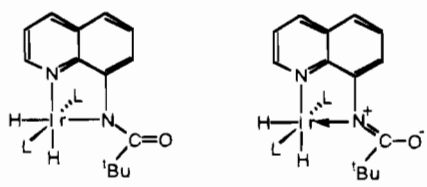

5 **5a**

The relatively low $\nu_{C=O}$ frequency (1594 cm^{-1}) in the IR spectrum indicates that the imino resonance form **5a** may be a significant contributor to the structure. The N → Ir bond shown in the diagram indicates the dative binding of the imino nitrogen lone pair in contrast to the covalent binding of the deprotonated amido nitrogen in **5**. This species, a rare example of an amido hydride complex, shows no sign of undergoing reductive elimination of the N−H bond.

Table 1. Crystallographic Data for $[Ir(H)_2(PPh_3)_2(C_9H_6N\{HNCO^tBu\})]SbF_6$ (**4b**) and $[Ir(H)_2(PPh_3)_2(C_9H_6N\{HNSi^tBuMe_2\})]SbF_6$ (**4c**)

	4b	**4c**
formula	$IrC_{50}H_{48}N_2OF_6P_2Sb$	$IrC_{51}H_{55}N_2P_2F_6SiSb$
fw	1215.8	1275.13
color and habit	colorless prism	colorless prism
crystal size, mm^3	0.10 × 0.10 × 0.15	0.20 × 0.24 × 0.36
crystal system	triclinic	monoclinic
a, Å	9.904(4)	45.24(1)
b, Å	13.480(5)	10.536(3)
c, Å	19.346(9)	25.450(7)
α, deg	83.79(4)	
β, deg	81.64(4)	111.11(2)
γ, deg	76.52(3)	
V, $Å^3$	2477(2)	11 318(10)
Z	2	8
space group	$P\bar{1}$	$C2/c$ (no. 15)
ρ_{calc}, g/cm^3	1.63	1.497
λ, Å (Mo Kα radiation)	0.710 73	0.710 73
μ, cm^{-1}	33.55	30.21
T, °C	17	−110
diffractometer	Siemens P4	Rigaku AFC5S
scan type	$\omega-2\theta$	$\omega-2\theta$
2θ range, deg	3−50	4.0−48.0
transm factors	0.9−1.0	0.83−1.00
rflns collected	8040	10 605
indpt rflns	7778	10 455
indpt obsvd rflns	5579 ($F_o \geq 4\sigma(F_o)$)	4198 ($I > 3\sigma(I)$)
R^a	0.054	0.053
$R_w{}^b$	0.057	0.058
goodness of fit^c	1.07	1.53

$^a R = \sum||F_o| - |F_c||/\sum F_o$. $^b R_w = [w\sum(|F_o| - |F_c|)^2/\sum wF_o^2)]^{1/2}$. ^{c} GOF $= [\sum w(|F_o| - |F_c|)^2/(N_o - N_v)]^{1/2}$.

Crystallographic Studies. The two most plausible alternative structures for **4**, the **A** or agostic form with an amide Ir···H−NR group and the **L** or lone-pair-bound form with an Ir−NHR group, are shown below.

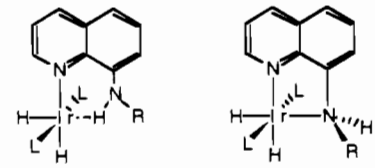

A **L**

Amine N lone pairs are basic and would be expected to give the **L** structure, but amide nitrogens, e.g., **2b**, are normally nonbasic and do not protonate or bind to metals, and silyl amines (**2c**) have low basicity.[7a] Neither **A** nor **L** structural types is known for amides (**2b**) or silyl amines (**2c**), so no literature data are available to help interpret the spectroscopic results. However, we were able to grow crystals of **4b**−**c** suitable for crystallographic study.

The crystal structure of **4b** (Tables 1 and 2 and Figure 1) shows that the amide group retains its amide form and has not tautomerized to an iminol as in the case of **3**.[6] The amide nitrogen is close enough to the metal to be considered as coordinated, but this bond is exceptionally long. The aromatic N has a normal Ir−N distance of 2.16 Å (typical range: 2.0−2.2 Å),[6a,7b,c] but the Ir−N distance involving the amide nitrogen is 2.313(9) Å. The crystal structure of **4c** (Tables 1 and 3 and Figure 2) shows a very similar situation with an Ir−N

(7) (a) Basch, H. *The Chemistry of Amides*; Zabicky, J., Ed.; Interscience: London, 1970; p 46. (b) Einstein, F. B. W.; Gilchrist, A. B.; Rayner-Ganham, G. W.; Sutton, D. *J. Am. Chem. Soc.* **1972**, *94*, 645. (c) Einstein, F. B. W.; Sutton, D. *J. Chem. Soc., Dalton. Trans.* **1973**, 436.

Table 2. Selected Bond Angles (Degrees) and Lengths (Angstroms) for $[Ir(H)_2(PPh_3)_2(C_9H_6N\{HNCO^tBu\})]SbF_6$ (**4b**)

Ir(1)−P(1)	2.303(3)	Ir(1)−P(2)	2.322(3)
Ir(1)−N(1)	2.159(8)	Ir(1)−N(2)	2.313(9)
N(2)−C(8)	1.465(13)	N(2)−C(10)	1.447(13)
O(1)−C(10)	1.190(13)	P(1)−Ir(1)−P(2)	161.6(1)
P(2)−Ir(1)−N(1)	91.0(2)	P(1)−Ir(1)−N(1)	93.7(2)
P(1)−Ir(1)−N(2)	95.3(2)	P(2)−Ir(1)−N(2)	103.1(2)
N(1)−Ir(1)−N(2)	77.4(3)	Ir(1)−N(2)−C(8)	107.0(6)
Ir(1)−N(2)−C(10)	112.5(7)	C(8)−N(2)−C(10)	114.5(8)
O(1)−C(10)−N(2)	121.4(8)	N(2)−C(8)−C(7)	119.6(9)

(silylamide) distance of 2.320(10) Å. In both cases, the Ir^{III} center has a distorted octahedral coordination with trans phosphines and cis hydrides as is known in many related structures.[8] The P−Ir−P angles are 161° and 158° for **4b** and **4c**, respectively. The $CO(^tBu)$ and $SiMe_2(^tBu)$ groups are canted with respect to the quinoline.

At this stage, the results do not allow us to choose unambiguously which of the possible structures, **A** or **L**, is present because the NH proton could not be located. The heavy atom positions allow two plausible assumptions for the N−H proton positions. If the amide N were sp^2, the N−H proton would be close to the metal, as expected for the **A** structure, or if the amide N were sp^3, the N−H proton could be distant from the metal, corresponding to the **L** structure. For example, if we assume an **A** structure for **4c** and take d(N−H) as 0.975 Å and ideal sp^2 angles for the substituted amine, we obtain a d(H···Ir) of 1.634 Å, entirely reasonable for an agostic structure.

Conventional NMR and IR Data. In the ^1H NMR spectrum of **4a** (Table 4) the two inequivalent Ir−H groups resonate as triplets of doublets as a result of coupling to the two *cis* PPh_3 (16 Hz) and one *cis* Ir−H (6 Hz), as expected for octahedral Ir^{III}. The ^{31}P NMR spectrum shows only one phosphine signal (24.1 ppm), as expected. There is an upfield shift of the NH proton, $\Delta\delta = -0.53$ ppm and a shift of ν(N−H) to lower energy (Table 5) in the IR (from 3453 and 3354 cm^{-1} of free ligand to 3296 and 3255 cm^{-1} of the complex, respectively). The equivalence of the two NH protons in **4a** precludes a structure such as Ir···H−N−H, assuming that we have a static structure. Consequently, we assign the **L** structure to **4a**. The complex will prove to be a useful model for discussion of the ^{15}N NMR results that follows. The proton NMR of **4b** is very similar to that of **4a**, but the NH proton is shifted even further upfield, $\Delta\delta = -3.70$ ppm, and the ^{31}P NMR now shows *two* PPh_3 signals at 23.6 and 26.0 ppm at 20 °C. Superficially, this seems to indicate the **L** structure, with its inequivalent PPh_3 groups, but even an **A** structure could give rise to inequivalence because agostic binding is side-on as shown below:

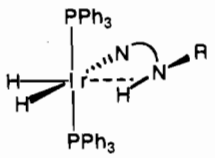

The $\nu_{C=O}$ IR band shifts from 1681 cm^{-1} in the free ligand to 1753 cm^{-1} in **4b**, suggestive of ketonic character. These data still did not allow a distinction between **A** and **L** structures, and so we carried out an ^{15}N NMR study.

Natural-Abundance ^{15}N NMR. ^{15}N NMR methods have been very useful[9] in connection with Pt···H−N interactions in that the one-bond coupling constant $^1J(^{15}N,^1H)$ is expected to be substantially reduced if the interaction with the metal is relatively strong (by analogy to M···CH agostic species).[1c]

^{15}N NMR data were successfully obtained on ligands **2a−c** and complexes **4a−c** (Table 4). We find $^1J(^{15}N,^1H)$ is substantially reduced on going from the free ligands to the Ir^{III} complexes, i.e., −89.2 to −74.1 Hz for **4b** and −76.3 to −62.6 Hz. For **4c**, there are also very large low-frequency coordination chemical shifts for the NH protons, e.g., 3.7 ppm for **4b**. At first sight, this seems to suggest that **4b** and **4c** do indeed contain agostic Ir···H−N interactions, but this analysis ignores the fact that these amino−quinoline ligands are related to anilines in which $^1J(^{15}N,^1H)$ values are normally somewhat larger than those for primary aliphatic amines owing to the delocalization of the aniline lone pair into the ring[10] and the consequent partial sp^2 character for the aniline nitrogen atom. In this light, the reduction in the $^1J(^{15}N,^1H)$ values becomes ambiguous since lone-pair coordination would involve rehybridizing nitrogen from pseudo-sp^2 to pseudo-sp^3 and a consequent reduction in $^1J(^{15}N,^1H)$. The marked upfield ^{15}N coordination chemical shifts are more in keeping[11] with a coordinated sp^3 nitrogen.

To distinguish definitively between the **A** and **L** structures, we obtained the $^2J(^{15}N,^1H\ \{hydride\})$ couplings between the amide N and the trans H, as shown below:

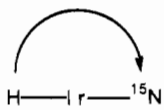

The only literature example of such a spin−spin coupling[12] was obtained from an ^{15}N-enriched sample. The natural-abundance study was greatly helped by the HMQC[13] experiments, which provide a theoretical enhancement of $(\gamma^{1H}/\gamma^{15N})^{5/2}$ relative to conventional 1-D measurements. The presence of a relatively large one-bond coupling constant makes the choice of delay time simple. The method is theoretically and practically much superior to 1-D work. It does, however, require some knowledge of J(N, H). Figure 3 shows the natural-abundance inverse $^1H,^{15}N\ \{^{31}P\}$ correlation for **4a**, where, as noted above, both nitrogens are presumed to be coordinated via the lone pair. From **4a** we obtained the necessary model $^2J(^{15}N,^1H\ \{hydride\})$ values as well as the appropriate ^{15}N chemical shifts. If both nitrogens of **4b** and **4c** are lone-pair bound, the trans spin−spin interaction should be substantial as the literature suggests.[14] Fortunately, complex **4a** is an excellent model, having $^2J(^{15}N,^1H\ \{hydride\})_{trans}$ values of 19 and 15 Hz for the quinoline and amino nitrogens, respectively. The analogous $^2J(^{15}N,^1H\ \{hydride\})_{trans}$ values for the amino nitrogens in **4b** and **4c** are both ca. 14 Hz. Further, we note the similarity of the $\Delta\delta^{15}N$ values in **4a−c**, strongly suggesting that the nitrogens in **4b−c** are indeed lone-pair bound to iridium.

(8) (a) Crabtree, R. H.; Hlatky, G. G.; Parnell, C. A.; Segmuller, B. E.; Uriarte, R. J. *Inorg. Chem.* **1984**, *23*, 354. (b) Luo, X.-L.; Crabtree, R. H. *Inorg. Chem.* **1990**, *29*, 682. (c) Crabtree, R. H.; Demou, P. C.; Eden, D.; Mihelcic, J. M.; Parnell, C.; Quirk, J. *J. Am. Chem. Soc.* **1982**, *104*, 6994.

(9) (a) Pregosin, P. S.; Rüegger, H.; Wombacher, F.; van Koten, G.; Grove, D. M.; Wehman-Ooyevaar, I. *Magn. Reson. Chem.* **1992**, *30*, 548. (b) Albinati, A.; Lianza, F.; Muller, B.; Pregosin, P. S. *Inorg. Chim. Acta* **1993**, *208*, 119. (c) Albinati, A.; Lianza, F.; Pregosin, P. S; Müller, B. *Inorg. Chem.* **1994**, *33*, 2522.

(10) Axenrod, T.; Pregosin, P. S.; Wieder, M. J.; Becker, E. D.; Bradley, R. B.; Milne, G. W. A. *J. Am. Chem. Soc.* **1971**, *93*, 6536.

(11) Moschi, H.; Pregosin, P. S.; Venanzi, L. M. *Helv. Chim. Acta* **1979**, *62*, 677. Appleton, T. G.; Bailey, A. J.; Barnham, K. J.; Hall, J. R. *Inorg. Chem.* **1992**, *31*, 3077.

(12) Koelliker, R.; Milstein, D. *Angew. Chem., Int. Ed. Engl.* **1991**, *30*, 707.

(13) (a) Kessler, H.; Ghurke, M.; Grieniger, C. *Angew. Chem., Int. Ed. Engl.* **1988**, *27*, 490. (b) Benn, R.; Gunther, H. *Angew. Chem., Int. Ed. Engl.* **1983**, *22*, 350.

(14) Pregosin, P. S.; Kunz, R. W. In *NMR Basic Principles and Progress*; Diehl, P., Fluck, E., Kosfeld, R., Eds.; Springer-Verlag: Berlin, 1979; Vol. 16, p 28.

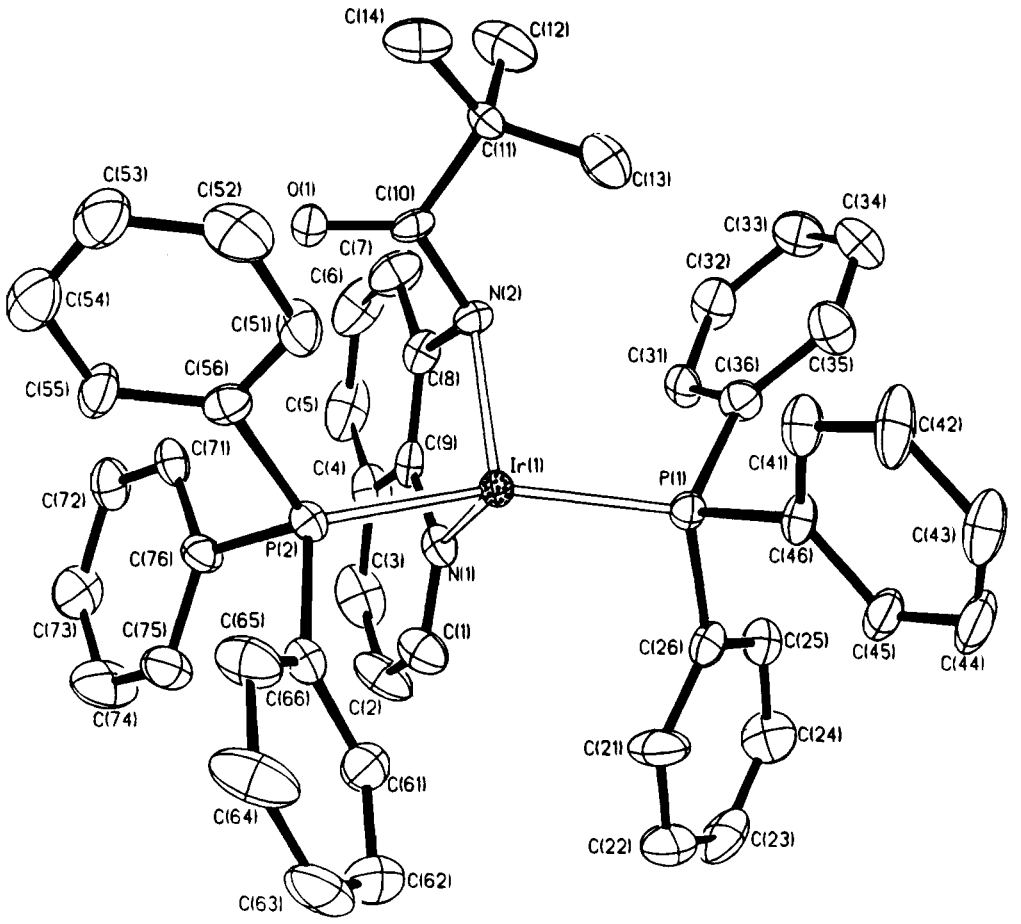

Figure 1. Diagram of the cation of $[Ir(H)_2(PPh_3)_2(C_9H_6N\{HNCO^tBu\})]SbF_6$ (**4b**). Thermal ellipsoids are at 50% probability. The hydrogen atoms have been omitted for clarity.

Table 3. Selected Bond Angles (Degrees) and Lengths (Angstroms) for $[Ir(H)_2(PPh_3)_2(C_9H_6N\{HNSi^tBuMe_2\})]SbF_6$ (**4c**)

Ir(1)−P(1)	2.335(5)	Ir(1)−P(2)	2.308(5)
Ir(1)−N(1)	2.18(1)	Ir(1)−N(2)	2.32(1)
N(2)−C(8)	1.48(2)	N(2)−Si	1.85(1)
Si−C(10)	1.86(2)	Si−C(11)	1.85(2)
P(1)−Ir(1)−P(2)	158.0(2)	P(2)−Ir(1)−N(1)	94.8(4)
P(1)−Ir(1)−N(1)	90.6(4)	P(1)−Ir(1)−N(2)	105.2(3)
P(2)−Ir(1)−N(2)	96.7(3)	N(1)−Ir(1)−N(2)	77.5(5)
Ir(1)−N(2)−C(8)	108.3(9)	Ir(1)−N(2)−Si	118.6(7)
C(8)−N(2)−Si	120(1)	N(2)−C(8)−C(7)	124(1)

NOESY. Any remaining doubt with respect to the structure of **4b** is removed by a ^1H NOESY study. The spectrum (Figure 4) shows a substantial NOE between the amide NH and H-7 of the quinoline.

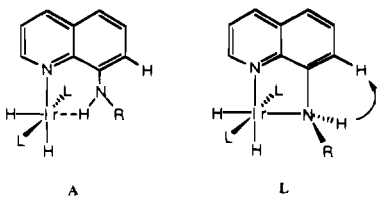

A L

This is reasonable only if **L** is the correct structure. Structure **L** is also consistent with the observation that at 243 K a strong selective NOE is found between the NH proton and only *one* of the PPh_3 ligands (from the meta protons), again consistent only with **L**. In connection with the 3-D solution structure of **4b**, we note a strong NOE between the ^{t}Bu methyl groups and the NH proton, suggesting that these two are relatively close in space and thus that the carbonyl group faces away from the NH toward a PPh_3 group in solution as indicated by the X-ray structure. Taken together, all the NMR data are consistent with N and not O (for **4b**) or N−H agostic coordination. The molecule therefore contains an example of an N-coordinated amide, of which there appears to be no previous example. A number of *apparent* examples of such binding are listed in the Cambridge database, but reference to the original papers shows that all these amides have sp^2 type planar nitrogens and are in fact deprotonated in the conventional manner; their structures are erroneously shown in the database.[15]

Fluxionality. Phase sensitive ^1H NOESY can afford both NOE and exchange information and, as shown for **4b** in Figure 5, at ambient conditions there is clearly *slow exchange* between the nonequivalent PPh_3 ligands (in this plot only the exchange cross-peaks together with the diagonal are shown). The hydride ligands do not exchange at this temperature, requiring an exchange mechanism in which these retain their coordination positions. PPh_3 dissociation and recoordination cannot be definitively excluded, but the five-coordinate intermediate would be likely to undergo a fluxional process, thereby probably exchanging the hydride ligands. It seems much more reasonable—especially given the long Ir−N(amino) distances—to suggest nitrogen dissociation, rotation, inversion at nitrogen, and recoordination via the lone pair.

At 20 °C, $[IrH_2(PPh_3)_2(C_9H_6N\{NH(Si^tBuMe_2)\})]SbF_6$ (**4c**) shows only one broad ^{31}P NMR phosphorus signal and one very broad ^1H NMR Si−Me signal. Upon cooling, the

(15) (a) Adams, H.; Bailey, N. A.; Briggs, T. N.; McCleverty, J. A.; Colquhoun, H. M.; Williams, D. J. *J. Chem. Soc., Dalton Trans.* **1986**, 813. (b) Brothers, P. J.; Clark, G. R.; Rickards, C. E. F. *J. Organomet. Chem.* **1992**, *433*, 203.

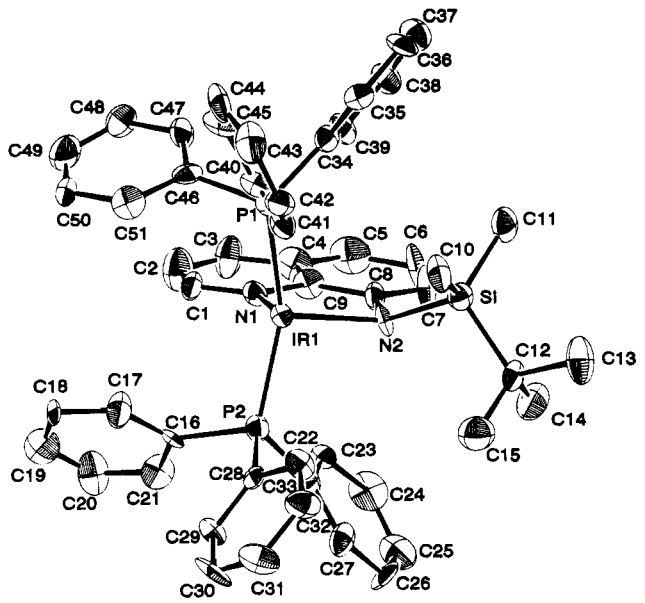

Figure 2. Diagram of the cation of $[Ir(H)_2(PPh_3)_2(C_9H_6N\{HNSi^tBuMe_2\})]SbF_6$ (**4c**). Thermal ellipsoids are at 50% probability. The hydrogen atoms have been omitted for clarity.

$SiMe_2$ groups decoalesced at 0 °C and gave two sharp peaks at −90 °C (0.39 and −0.88 ppm). These observations are only consistent with the N inversion mechanism described above.

Ir−N Bond Energy. The barrier for the fluxional process in **4c**, 14 kcal/mol, would normally be identified with the Ir−N bond energy. However, we suggest that the true bond energy may be substantially higher than this if an N−H···Ir agostic species is an intermediate in the process, thereby avoiding a completely decoordinated amide. Rotation of the −NHR group into the plane of the arene is known to lead to a resonance stabilization of ca. 5.8 kcal/mol.[16] Assuming a plausible[1a,c] agostic interaction strength of 15 kcal/mol, the true Ir−N bond energy would be in the range 30−35 kcal/mol. The analogous barrier for **4b** cannot be determined, but it must be >16 kcal/mol (no coalescence for ^{31}P signals at 65 °C). For the amide complex, **4b**, the exchange mechanism could involve reversible migration of the amide NH proton to the carbonyl oxygen to give the iminol tautomer, which would also allow nitrogen inversion to take place.

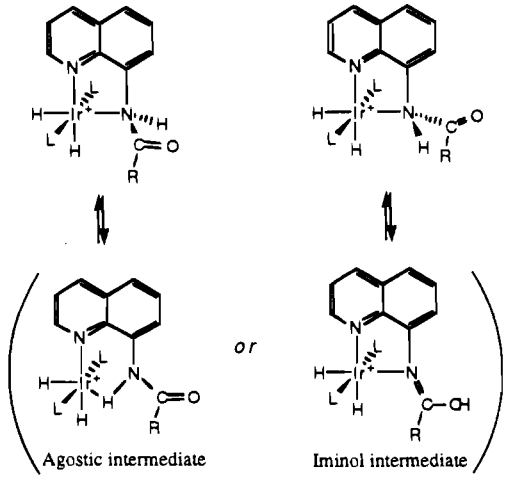

(16) Peris, E.; Lee, J. C., Jr.; Rambo, J. R.; Eisenstein, O.; Crabtree, R. H. *J. Am. Chem. Soc.* **1995**, *117*, 3485.

Conformationally Restricted System. We have also studied ligand **6**, in which the N−H bond cannot rotate and where lone-pair binding can therefore be ruled out. This only gave NH deprotonation to form the neutral complex **7** on reaction with **1**. This result suggests that when an agostic intermediate is formed, it loses a proton very easily. The addition of acid to **7** failed to reprotonate the system to yield an N−H agostic species. This is consistent with the strong acidification (ca. 20 pK units) of X−H bonds that has been noted[1c] for agostic binding (X = C or H). A free N−H bond, being much more acidic than a free C−H or H−H bond, more easily loses a proton on binding.

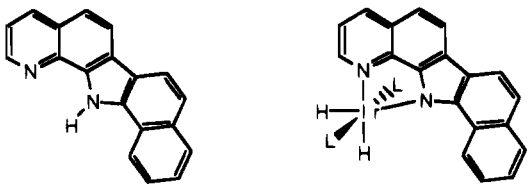

6 **7**

III. Conclusion

The full characterization of the novel species **4b−c** proved to be possible only by combining spectroscopic and structural studies. A key piece of evidence comes from the ^{15}N studies, which, in contrast to most previous cases, were performed at natural abundance. We conclude that in all the species the N lone pair, not the N−H bond, is bound to iridium. For **4b**, this represents the first known example of an undeprotonated amide coordinated via nitrogen and not oxygen. The low value of the barrier for N decoordination and inversion is consistent with (but does not definitely prove) the presence of an agostic intermediate. In ligand **6**, where lone-pair binding is excluded by the rigid conformation of the ring system, only N−H deprotonation is seen rather than the formation of a stable agostic system. Isolation of N−H agostic systems may still be possible if proton loss can be prevented by choosing a less electrophilic metal complex than **1** or a less acidic amine than **6**.

It is sometimes assumed that to form a complex of a deprotonated amide, it is necessary first to deprotonate the amide. Therefore, a strong base is commonly chosen. The conversion of **4b** to **5** shows that the amide can in fact first bind to the metal via the lone pair, making the NH proton much more acidic so that it can be deprotonated by a much weaker base, in this case, NEt_3.

IV. Experimental Section

General Procedures and Materials. All reactions were performed under a dry, oxygen-free nitrogen atmosphere using standard Schlenk techniques. All solvents were dried appropriately before use. ^1H chemical shifts (δ, ppm) were measured relative to TMS, ^{31}P shifts relative to external H_3PO_4, and ^{15}N shifts relative to external CH_3NO_2. NMR spectra were recorded on a Bruker AMX 500 instrument at ETH operating at 500.13 (^1H), 50.68 (^{15}N), and 202.46 (^{31}P) MHz, respectively, or a GE Omega-300 at Yale. The ^1H NOESY data were obtained using standard pulse sequences and a mixing time of 0.8 s. Typically, 1024 increments of size 2K (32 scans each) were acquired (covering both the hydride and conventional regions). $^{15}N,^1H$-HMQC experiments, to determine $^1J(^{15}N,^1H)$, were carried out using standard pulse sequences. To center on the proper ^{15}N frequency, a trial spectrum of 64 increments (with 64 scans each) [F1 (^{15}N)] of size 4K [F2 (^1H)] was recorded (200 and 10 ppm, respectively). The spin evolution time (1/2J) was chosen to be 6 ms. The final spectrum was acquired with a 10 ppm window in F1 and a refined spin evolution time according to the observed $^1J(^{15}N,^1H)$. The $^{15}N,^1H\{^{31}P\}$-HMQC experiments, to determine $^2J(^{15}N,^1H)$, were conducted on a triple resonance inverse probe head. The standard pulse sequence for the $^{15}N,^1H$-HMQC

Table 4. Selected ^1H, ^{31}P, and ^{15}N NMR Data for Compounds **2a**−**c** and **4a**−**c** in CD_2Cl_2[a]

	2a	4a	2b	4b	2c	4c
			^1H NMR			
δ H−Ir−$N_{(amino)}$		−19.90		−19.67		−19.78
δ H−Ir−$N_{(quinoline)}$		−20.77		−24.40		−23.39
$^2J(^1H,^{31}P)_{cis}$		16.0		18.0		19.8
$^2J(^1H,^1H)_{cis}$		6.0		7.1		8.4
δ HN	5.09	4.56	10.24	6.54	6.31	4.19
H7	6.92	7.23	8.76	7.06	6.97	7.22
			^{31}P NMR			
δ ^{31}P		24.1		26.0/23.6		23.9/21.0
$^2J(^{31}P,^{31}P)$				337		351
			^{15}N NMR			
$\delta(^{15}N)$	−329.2	−372.6	−263.2	−304.6	−323.5	−377.4
$^1J(^1H,^{15}N)$	−83.2	−72.2	−89.2	−74.1	−76.3	−62.6
$^2J(^1H,^{15}N_{amino})$		−15 ± 1		−14 ± 1		−15 ± 1
$^2J(^1H,^{15}N_{quinoline})$		−19 ± 1		−20 ± 2		−19 ± 1

[a] Spectra for **2a**, **4a**, 2b, and **4b** were acquired at room temperature but for **2c** and **4c** at 243 K.

Table 5. Selected IR Data for Compounds **2a**−**c** and **4a**−**c** (in cm^{-1})[a]

	2a	4a	2b	4b	2c	4c
ν(N−H)	3453 3354	3296 3255	3365	3245	3324	3207
ν(Ir−H)		2173		2184 2279		2248
ν(C=O)			1681	1753		

[a] In nujol mull.

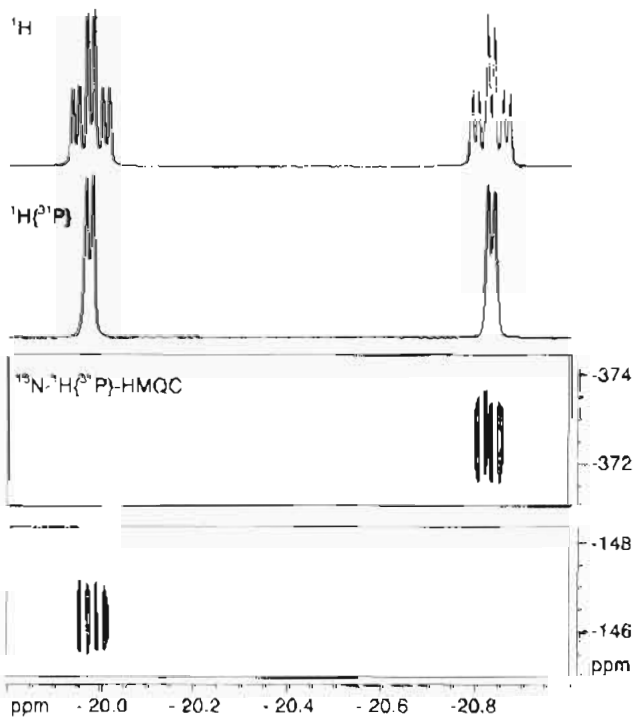

Figure 3. Natural-abundance ^1H,^{15}N $\{^{31}P\}$ HMQC correlation for **4a** (lower two traces, showing the two different N absorptions). Shown are the ^1H spectrum for **4a** in the hydride region (upper trace) and the ^1H spectrum for **4a** in the hydride region with ^{31}P decoupling, thereby revealing ^2J(H,H) (middle trace).

experiment was altered to permit ^{31}P decoupling using a WALTZ 16 sequence covering 2000 Hz. Typically, 32 increments (with 64 scans each) of size 8K were sampled. IR spectra were recorded on a MIDAC M1200 FTIR spectrometer.

$[IrH_2(acetone)_2(PPh_3)_2]SbF_6$ (**1**) was obtained according to literature methods.[7c] 8-Aminoquinoline, *tert*-butyldimethylsilyl chloride, and butyllithium (Aldrich) were used as received. Ligands **2b** and **6** were prepared according to literature methods.[7a,17]

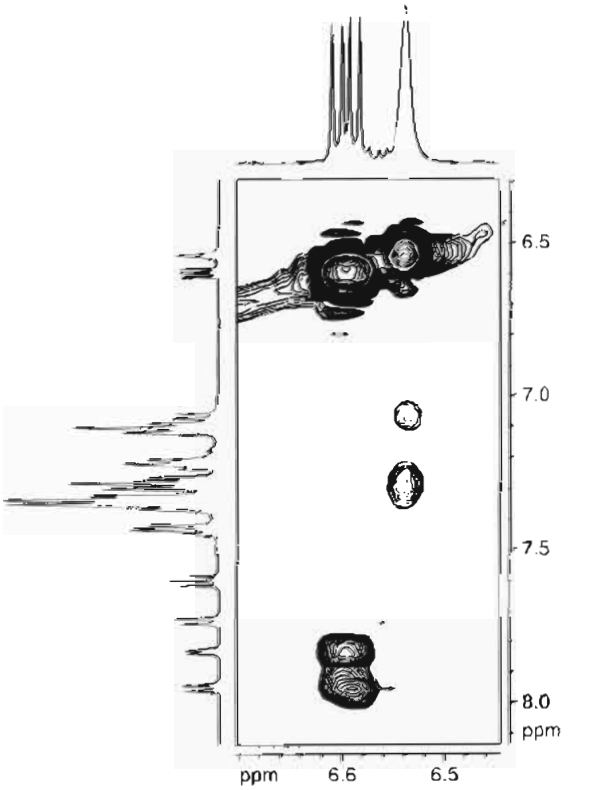

Figure 4. Section of the ^1H NOESY spectrum for **4b** (243 K, CD_2Cl_2) showing key NOEs from the NH proton (broad signal on the horizontal axis) to H-7, δ = 7.06 (moderate NOE), as well as to one of the two nonequivalent sets of meta protons at δ = 7.28 (strong NOE).

X-ray Experimental Section. Suitable crystals are grown by layering a CH_2Cl_2 solution of **4b** or **4c** with supernatant hexanes. The solid-state structures were determined by application of general procedures described elsewhere.[18,19] Crystal and experimental data are summarized in Table 1. Atomic coordinates, equivalent isotropic displacement coefficients, complete tables of bond distances and angles, and anisotropic displacement coefficients are available as supplementary material.

Structure Determination of 4b. A suitable crystal for single-crystal X-ray diffraction was selected and mounted in a nitrogen-flushed, thin-walled capillary tube. The unit-cell parameters were obtained by the least-squares refinement of the angular settings of 25 reflections (20°

(17) Buu-Hoi, N. P.; Perin, F.; Jacquignon, P. *J. Chem. Soc.* **1962**, 146.
(18) Loza, M. L.; De Gala, S. R.; Crabtree, R. H. *Inorg. Chem.* **1994**, *33*, 5073.
(19) Du, Y.; Rheingold, A. L.; Maatta, E. A. *Inorg. Chem.* **1994**, *33*, 6415.

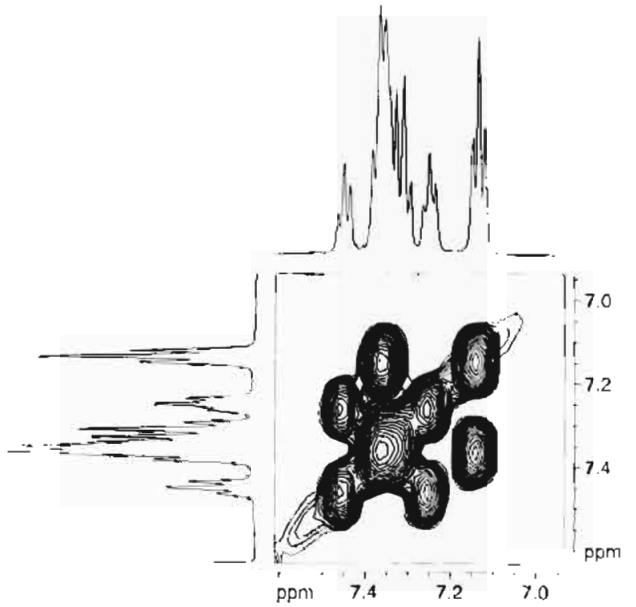

Figure 5. Section of the ambient temperature, phase-sensitive NOESY spectrum for **4b** showing the exchange between the two different meta and two different para protons coming from the nonequivalent PPh_3 ligands.

$\leq 2\theta \leq 25°$). No evidence of symmetry higher than triclinic was observed in either the photographic or diffraction data. Semiempirical absorption corrections were applied to the data. E-statistics suggested a centrosymmetric space group, and $P\bar{1}$ was chosen and subsequently verified by chemically reasonable results of refinement. The following octants were collected: $\pm h,\pm k,+l$. The structure was solved by direct methods, completed by subsequent difference Fourier syntheses and refined by full-matrix least-squares procedures. All non-solvent, non-hydrogen atoms were refined with anisotropic displacement coefficients. Ligand hydrogen atoms were treated as idealized contributions. The hydride ligand atom was not located in the difference map and was ignored. All software and sources of the scattering factors are contained in either the SHELXTL (5.1) or the SHELXTL PLUS (4.2) program libraries (G. Sheldrick, Siemens XRD, Madison, WI).

Structure Determination of 4c. A suitable crystal was mounted on a glass fiber. The unit-cell parameters were obtained by the least-squares refinement of 15 carefully centered reflections in the range $7.22 < 2\theta < 15.28°$. The following octants were collected: $+h,+k,\pm l$. An empirical absorption correction based on azimuthal scans of several reflections was applied, which resulted in transmission factors ranging from 0.83 to 1.00. The data were corrected for Lorentz and polarization effects. The structure was solved by a combination of the Patterson method and direct methods. The non-hydrogen atoms were refined anisotropically. Ligand hydrogen atoms were treated as idealized contributions. The hydride ligand atom was not located in the difference map and was ignored (see **4b** for software and sources of the scattering factors).

Preparation of Ligand 2c. To 8-aminoquinoline (430 mg, 2.98 mmol) in CH_2Cl_2 (20 mL) were added 1.05 equiv of ^nBuLi (2.0 M in cyclohexane) and then $Me_2{}^tBuSiCl$ (448 mg, 2.98 mmol) with stirring; the mixture was then stirred for 5 h. The resulting suspension was filtered on a 5 cm Celite column and the filtrate purified by chromatography (Basic Alumina, 80−200 mesh) with CH_2Cl_2 as eluent. Removal of solvent from the eluate from the first yellow band gave **2c** as yellow oil (86%). ^1H NMR (CD_2Cl_2, δ): 0.35 (s, 6H, $SiMe_2$); 1.05 (s, 9H, ^tBu); 6.31 (s, 1H, NH); 6.95; 7.09; 7.31; 7.37; 8.07; 8.73 (aromatic protons). IR (nujol, cm^{-1}): 3324 (w, ν_{N-H}).

Preparation of Complexes of Type 4. Typical Procedure. To a stirred solution of complex **1** (150.0 mg, 0.140 mmol) in CH_2Cl_2 (4 mL) was added 8-aminoquinoline (20.2 mg, 0.140 mmol). After 3 min at room temperature, a pale yellow solution was formed, which was concentrated to ca. 1 mL and diethyl ether (2 mL) added to give **4a** as an off-white solid (122 mg, 79%) that was recrystallized from CH_2Cl_2/hexanes. ^1H NMR (CD_2Cl_2, δ): 4.56 (s, 2H, NH_2); −19.90 (td, 1H, $^2J(P,H) = 16.0$ Hz, $^2J(H,H) = 6.0$ Hz); −20.77 (td, 1H, $^2J(P,H) = 16.0$ Hz, $^2J(H,H) = 6.0$ Hz); 7.23−7.42 (m, 30H, PPh_3); 8.01; 7.88; 7.65; 7.42; 7.23; 6.63 (6H, aromatic protons). $^{31}P\{^1H\}$ NMR (CD_2Cl_2, δ): 24.1 (s). IR (nujol, cm^{-1}): 3296.0, 3255.1 (m, ν_{N-H}), 2171.3 (w, ν_{Ir-H}). Anal. Calcd for $C_{45}H_{40}IrN_2P_2SbF_6$: C, 49.19; H, 3.67; N, 2.55. Found: C, 48.83; H, 3.35; N, 2.78.

Compound **4b** was prepared similarly as an off-white solid in 67% yield. ^1H NMR (CD_2Cl_2, δ): 6.54 (s, 1H, NH); −19.67 (td, 1H, $^2J(P,H) = 18.0$ Hz, $^2J(H,H) = 7.1$ Hz); −24.40 (td, 1H, $^2J(P,H) = 18.0$ Hz, $^2J(H,H) = 7.1$ Hz); 7.12−7.55 (m, 30H, PPh_3); 7.95; 7.83; 7.73; 7.60; 7.06; 6.60 (6H, aromatic protons). $^{31}P\{^1H\}$ NMR (CD_2Cl_2, δ): 23.6 (d, $^2J_{(31P,31P)} = 337$ Hz); 26.0 (d, $^2J_{(31P,31P)} = 337$ Hz). IR (nujol, cm^{-1}): 3245 (m, ν); 2184; 2279 (w, ν_{Ir-H}); 1753 (s, $\nu_{C=O}$). Anal. Calcd for $C_{50}H_{48}IrN_2OP_2SbF_6$: C, 50.77; H, 4.09; N, 2.37. Found: C, 50.42; H, 4.31; N, 2.10.

Compound **4c** was prepared similarly in 75% yield. ^1H NMR (CD_2Cl_2, δ): 4.19 (s, 1H, NH); −19.78 (td, 1H, $^2J(P,H) = 19.8$ Hz, $^2J(H,H) = 8.4$ Hz); −23.39 (td, 1H, $^2J(P,H) = 19.8$ Hz, $^2J(H,H) = 8.4$ Hz); 6.88−7.33 (m, 30H, PPh_3); 8.06; 7.81; 7.60; 7.22; 6.81; 6.52 (6H, aromatic protons). $^{31}P\{^1H\}$ NMR (CD_2Cl_2, δ): 22.5 (br). IR (nujol, cm^{-1}): 3207.2 (m, ν_{N-H}), 2247.6 (w, ν_{Ir-H}). Anal. Calcd for $C_{51}H_{55}IrN_2P_2SbSiF_6$: C, 50.46; H, 4.57; N, 2.31. Found: C, 50.12; H, 4.78; N, 2.08.

Deprotonation of 4b. Formation of 5. To a stirred solution of **4b** (55 mg, 0.047 mmol) in CH_2Cl_2 (2mL) was added Et_3N (6.3 μL). After 10 min stirring at 20 °C, the solution was concentrated to ca. 1 mL and diethyl ether (2mL) was added to give **5** as an orange solid (28 mg, 64%). ^1H NMR (CD_2Cl_2, δ): −18.97 (td, 1H, $^2J(P,H) = 18.0$ Hz, $^2J(H,H) = 7.2$ Hz); −21.68 (td, 1H, $^2J(P,H) = 18.0$ Hz, $^2J(H,H) = 7.2$ Hz); 7.14−7.51 (33H, aromatic protons); 7.09; 6.71; 6.12 (3H, aromatic protons). $^{31}P\{^1H\}$ NMR (CD_2Cl_2, δ): 21.12 (s). IR (nujol, cm^{-1}): 2193; 2141 (w, ν_{Ir-H}); 1594 (m, $\nu_{C=O}$). Anal. Calcd for $C_{50}H_{47}IrON_2P_2$: C, 63.48; H, 5.01; N, 2.96. Found: C, 63.15; H, 4.83; N, 3.21.

Synthesis of Complex 7. To a stirred solution of complex **1** (100.0 mg, 0.093 mmol) in CH_2Cl_2 (3 mL) was added **6** (25.0 mg, 0.093 mmol). After 20 min at room temperature, a yellow suspension was formed. The resulting suspension was filtered on a 5 cm Celite column, and the filtrate was concentrated to ca. 1 mL and diethyl ether (2mL) added to give **7** as a yellow solid (122 mg, 79%). ^1H NMR (CD_2Cl_2, δ): −19.35 (td, 1H, $^2J(P,H) = 16.5$ Hz, $^2J(H,H) = 6.3$ Hz); −20.25 (td, 1H, $^2J(P,H) = 16.5$ Hz, $^2J(H,H) = 6.3$ Hz); 6.80−8.10 (41H, aromatic protons); 9.78; 6.61 (2H, aromatic protons). $^{31}P\{^1H\}$ NMR (CD_2Cl_2, δ): 28.41 (s). Anal. Calcd for $C_{53}H_{43}IrN_2P_2$: C, 66.99; H, 4.40; N, 2.84. Found: C, 66.68; H, 4.68; N, 3.04.

Acknowledgment. We thank the U.S. National Science Foundation, the Swiss National Science Foundation, and Exxon Corp. for funding and Dr. H. Rüegger for helpful discussions.

Supporting Information Available: X-ray characterization data for complexes **4b** and **4c** including tables of detailed crystallographic data, atomic coordinates, H-atom coordinates, anisotropic displacement coefficients, bond lengths, and bond angles (23 pages). This material is contained in many libraries on microfiche, immediately follows this article in the microfilm version of the journal, and can be ordered from the ACS; see any current masthead page for ordering information.

IC941485T